

Secure Federated Learning for Neuroimaging

Dimitris Stripelis, Umang Gupta, Hamza Saleem, Nikhil Dhinagar, Tanmay Ghai, Rafael Sanchez, Chrysovalantis Anastasiou, Armaghan Asghar, Greg Ver Steeg, Srivatsan Ravi, Muhammad Naveed, Paul M. Thompson, José Luis Ambite,

Abstract—The amount of biomedical data continues to grow rapidly. However, the ability to collect data from multiple sites for joint analysis remains challenging due to security, privacy, and regulatory concerns.

We present a *Secure Federated Learning* architecture, MetisFL, which enables distributed training of neural networks over multiple data sources without sharing data. Each site trains the neural network over its *private data* for some time, then shares the neural network parameters (i.e., weights, gradients) with a Federation Controller, which in turn aggregates the local models, sends the resulting community model back to each site, and the process repeats.

Our architecture provides *strong security and privacy*. First, sample data never leaves a site. Second, neural parameters are encrypted before transmission and the community model is computed under *fully-homomorphic encryption*. Finally, we use information-theoretic methods to *limit information leakage* from the neural model to prevent a “curious” site from performing membership attacks.

We demonstrate this architecture in *neuroimaging*. Specifically, we investigate training neural models to classify Alzheimer’s disease, and estimate Brain Age, from magnetic resonance imaging datasets distributed across multiple sites, including heterogeneous environments where sites have different amounts of data, statistical distributions, and computational capabilities.

Index Terms—Federated Learning, Deep Learning, Privacy, Security, Alzheimer’s Disease, Brain Age, Magnetic Resonance Imaging, Membership Attacks.

I. INTRODUCTION

Deep learning and traditional machine learning methods are now widely applied across biomedical research [1]. These methods have been particularly successful in medical imaging [2], including image reconstruction and enhancement [3],

This research was supported in part by the Defense Advanced Research Projects Agency (DARPA) under contract HR00112090104, and in part by the National Institutes of Health (NIH) under grants U01AG068057 and RF1AG051710. This is a study of previously collected, anonymized, de-identified data, available in a public repository. Data access approved by UK Biobank under Application Number 11559.

DS, UG, HS, TG, RS, CA, AA, GVS, SR, MN, and JLA are with the Computer Science Department, University of Southern California, Los Angeles, 3551 Trousdale Pkwy, CA 90089.

DS, UG, TG, RS, CA, AA, GVS, SR, and JLA are also with the Information Sciences Institute, University of Southern California, 4676 Admiralty Way, Marina del Rey, CA 90292.

ND and PMT are with the Imaging Genetics Center, Stevens Neuroimaging and Informatics Institute, University of Southern California, 4676 Admiralty Way, Marina del Rey, CA 90292.

Emails: stripeli@isi.edu, umanggup@usc.edu, hsaleem@usc.edu, dhinagar@usc.edu, tghai@isi.edu, rafsan@isi.edu, canastas@usc.edu, aasghar@usc.edu, gregv@isi.edu, sravi@isi.edu, mnaveed@usc.edu, pthomp@usc.edu, ambite@isi.edu

automated segmentation and labeling of key structures [4], computer aided diagnosis [5], pathology detection [6], disease subtyping [7], [8], and predictive analytics (e.g., modeling future recovery or decline) [9]. In neuroimaging, there is great progress in automated diagnostic classification and subtyping of diseases, such as Alzheimer’s disease and Parkinson’s disease, to assist in patient management and monitoring, and to screen patients for eligibility for clinical trials. Some recent MRI-based classifiers have merged data from over 80,000 individuals for diagnostic classification [10].

The performance of deep learning methods depends heavily on the availability of large amounts of training data. Unfortunately, for many areas of biomedical research, such as neuroimaging, data acquisition is expensive. Therefore, any single organization or research group is only able to collect a limited amount of data.

To increase the amount of data and statistical power of analyses, research groups join together into consortia [11]. However, the need to protect patient data makes data sharing very challenging. Regulatory frameworks, such as the *Health Insurance Portability and Accountability Act* (HIPAA), require strict protection of health records and data collected for medical research. Privacy laws have spurred research into anonymization methods; for example, algorithms to remove facial information from MRI scans [12]–[14]. The inherent complexity and cost of enforcing security and privacy results in few large-scale data sharing efforts. Even when large consortia are established, they often only perform meta-analysis using traditional statistical methods, as opposed to joint mega-analysis using deep learning methods. A paradigmatic example of large-scale meta-analysis is the ENIGMA Consortium [11].

Federated Learning [15]–[17] has emerged as a novel distributed machine learning paradigm that enables large-scale cross-institutional analysis without the need to move the data out of its original location. Federated Learning allows institutions to collaboratively train a machine learning model (e.g., a neural network) by aggregating the parameters (e.g., weights, gradients) of local models trained on local data. Since subject data is not shared, and parameters can be protected through encryption, privacy concerns are ameliorated. Federated Learning is being increasingly applied in biomedical and healthcare domains [18]–[22].

In this paper, we present our *Secure Federated Learning* architecture as an end-to-end solution to neural network training across data silos. Our architecture is extensible and supports a variety of training policies that perform well across heterogeneous environments, where sites have different

amounts of data, statistical distributions, and computational capabilities, which is often the case in biomedical research applications. Our architecture provides *strong security and privacy guarantees*. Data is never shared. Model parameters are transmitted through secure communication channels. Moreover, model parameters are encrypted and the community model is computed under fully-homomorphic encryption (using CKKS [23]), so even if the controller was compromised the community model cannot be attacked. Finally, we use information-theoretic methods to *limit information leakage* from the neural model to prevent a "curious" site from performing model inversion or membership attacks. Our main contributions are:

- A modular and extensible Federated Learning architecture to enable secure and private distributed analysis across data silos (Section II).
- An encrypted communication and aggregation training protocol based on fully-homomorphic encryption, which enforces security, while maintaining learning performance with a moderate computational cost (Section IV).
- Information-theoretic protection methods against model inversion and membership attacks (Section V).
- An detailed evaluation of convolutional neural models in statistically and computationally heterogeneous federated learning environments for two neuroimaging tasks: prediction of Alzheimer's Disease, and of Brain Age, from MRI scans (Section IV).

II. FEDERATED LEARNING

We describe the Federated Learning problem, our architecture, and federated training policies.

A. Federated Optimization

A federated learning environment consists of N learners (clients, sites) that jointly train a machine learning model, often a neural network. The goal is to find the model parameters w^* that optimize the global objective function $F(w)$:

$$w^* = \underset{w}{\operatorname{argmin}} F(w) = \sum_{k=1}^N \frac{p_k}{\mathcal{P}} F_k(w)$$

where $F_k(w)$ denotes the local objective function of learner $k \in N$ optimized over its local training dataset D_k .

The global model, $F(w)$, is computed as a weighted average of the learners' local models, $\mathcal{P} = \sum_k |p_k|$. A typical policy, which we follow in this paper, is to weigh each local model based on the number of training examples it was trained on, i.e., $p_k = |\mathcal{D}_k|$ [15], though other methods are possible [16], [24], [25]. Each learner uses Stochastic Gradient Descent (SGD) to optimize its local objective on its local dataset. At a given synchronization point, each learner shares its local model parameters with the Federation Controller, which aggregates the local models (e.g., using weighted average) to compute a global (or community) model, sends it back to the learners, and the process repeats. Each such cycle is called a federation round. This iterative process was first introduced in the seminal work of [15] and it is termed as *FedAvg*. More recent works [26]–[28] have proposed a more

general federated learning optimization framework where the optimization problem is split into global (server-side) and local (client-side). Global targets to optimize the merging rule of the learners' models updates into the global model and local targets to optimize learners' local training. During training a learner only shares its local model parameters with the Federation Controller. Each local dataset remains private.

B. Secure Federated Architecture: MetisFL

We have developed a modular, extensible, secure federated learning system, called *MetisFL* [29], that can support arbitrary training policies, in addition to enforcing privacy and security. The architecture consists of three main entities, the federation driver, the federation controller and the learner. Figure 1 provides a detailed overview of all the architecture and its micro-services. The driver is a trusted entity and it is the entry point of the federation, which is responsible for initializing and shutting down the controller and learner services at the remote hosts, defining the machine learning model architecture, initializing the model's original state, and generating the public and private keys required for homomorphically encrypted communication and global aggregation (see Section IV). The controller is responsible for orchestrating the execution of the federated model across the participating learners by synchronizing learners' local models according to the communication protocol being employed, scheduling the local training task to each learner, and aggregating the (encrypted or non-encrypted) local models of the learners to compute the new global (community) model. The learner is responsible for receiving the global model from the controller, evaluating or training (with or without information guarantees) the global model on its private local dataset according to the task delegated by the controller, and sending its locally evaluated or trained model back to the controller. Finally, the communication across all services is established using the gRPC protocol and the backend neural network training engine currently used is Tensorflow; even though our architecture is extensible and can support additional engines as well. The architecture is containerized to facilitate deployment.

C. Federated Training Policies

During federated training, the communication between the learners and the controller may follow a synchronous [15], [30], asynchronous [31], or semi-synchronous [29] protocol. During synchronous training, the controller needs to wait for all learners to complete their local training task before a new global model is computed, while during asynchronous training, whenever a single learner completes its local training task a new global model is computed by the controller. Even though synchronous training improves model performance at the expense of resource under-utilization (e.g., idle time), asynchronous training improves resource utilization but reduces model performance. To balance this trade-off, our semi-synchronous protocol [29], [32] allocates more local training steps to computationally fast learners instead of leaving them idle. The synchronization period of the semi-synchronous protocol is based on the time required by the slowest learner in

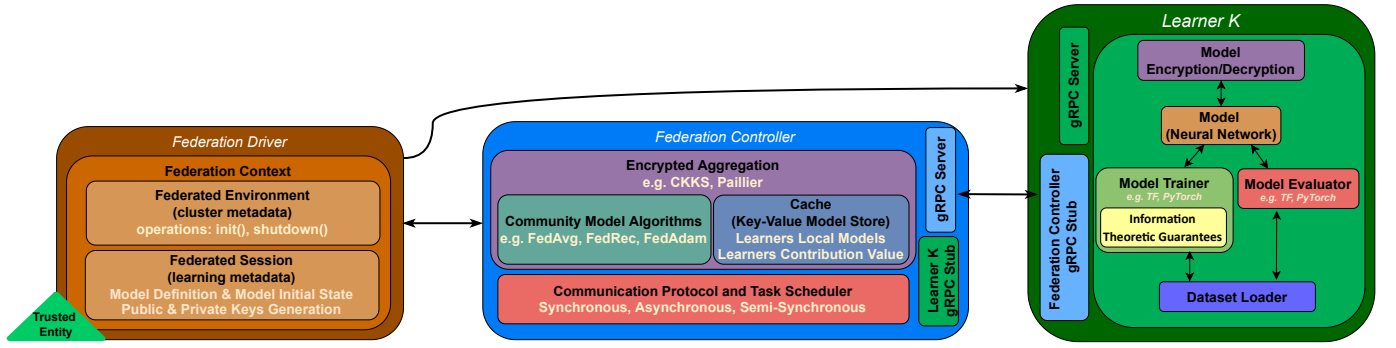


Fig. 1: Metis Federated Learning Framework Architecture.

the federation to complete a single epoch on its local dataset. The length of this period is controlled by a hyperparameter λ , which is used by the controller to estimate and delegate the respective number of local training steps to each learner.

III. FEDERATED LEARNING IN NEUROIMAGING

We have applied our MetisFL architecture to two learning tasks in neuroimaging: a regression problem, predicting BrainAGE, and a classification problem, predicting Alzheimer's disease status, both on structural MRI inputs.

A. Predicting BrainAGE

The Brain Age Gap Estimation (BrainAGE) task uses structural MRI scans to assess acceleration or deceleration of an individual's brain aging. The difference between the true chronological age and the predicted age of the brain is considered an important biomarker for early detection of age-associated neurodegenerative and neuropsychiatric diseases [33], [34], such as cognitive impairments [35], schizophrenia [36], chronic pain [37]. Recently, deep learning methods based on RNN [38], [39] and CNN [40]–[43] architectures have demonstrated accurate brain age predictions.

We extended these methods to train a 3D-CNN model over a federation with highly heterogeneous data distributions [29], [32]. Below we report experiments on the same 3D-CNN architecture as in [32], but without the dropout layer. This slight modification improved the learning performance on the BrainAGE task for both the centralized and federated models across all environments. The training and testing datasets follow [29], [32]. We selected 10,446 scans (out of 16,356) from the UKBB [44] dataset with no indication of neurological pathology, and no psychiatric diagnosis as defined by the ICD-10 criteria. All scans were evaluated with a manual quality control procedure and processed using a standard preprocessing pipeline with non-parametric intensity normalization for bias field correction and brain extraction using FreeSurfer and linear registration to a $(2 \text{ mm})^3$ UKBB minimum deformation template using FSL FLIRT. The final dimension of each scan was $91 \times 109 \times 91$. Of the 10,446 scans, we used 8356 for training and 2090 for testing.

We generated four computationally and statistically heterogeneous federated learning environments comprising eight learners. Computationally, the first four learners were equipped

with NVIDIA GeForce GTX 1080 Ti GPUs, while the last four had (faster) Quadro RTX 8000 GPUs. Figure 2 shows the four environments with diverse data amount and data distributions. For data amounts, we considered both *Uniform*, equal number of training samples per learner, and *Skewed*, decreasing amount of training samples for each learner. For data distributions, we considered both *Independent and Identically Distributed (IID)*, the local data distribution of each learner contains scans with the same distribution as the global age distribution, and *Non-IID*, different age distributions.

The learning performance of several synchronous, asynchronous, and semi-synchronous federated training protocols for these heterogeneous environments appears in Figure 3. We tested synchronous (SyncFedAvg), asynchronous (AsyncFedAvg), and semi-synchronous (SemiSyncFedAvg) federated training policies, all using the data size as a weighting rule (cf. Section II-C). Each learner trained using SGD with a learning rate of 5×10^{-5} and a batch size of 1. For SyncFedAvg and AsyncFedAvg, local training was for 4 epochs. For SemiSyncFedAvg we evaluated synchronization periods λ equivalent to the time it took the slowest learner to complete 4 or 2 epochs. AsyncFedAvg uses the caching method we introduced in [29], which significantly improves performance. The controller stores the most recently committed local model of each learner into a cache. When a learner issues an update request, the controller replaces its previously cached model and computes the new global model by performing a weighted average using all cached models.

We compare the learning convergence of the training policies based on elapsed execution (wall-clock) time (Figure 3a), and communication cost (models exchanged) (Figure 3b). A centralized model trained over all the data achieves a Mean Absolute Error (MAE) of 2.7 (shown as a horizontal line). In IID environments, both for Uniform and Skewed data amounts, federated training achieves comparable learning performance (MAE) to centralized training. However, in Non-IID environments a performance gap appears. The best performing federated training policy is our SemiSync ($\lambda = 4$) with MAE of 2.9 for Uniform & Non-IID and 3.1 for Skewed & Non-IID, which also shows a slightly faster convergence rate. The asynchronous protocol, AsyncFedAvg, is competitive on task performance, but it requires significantly more communication (models exchanged). SemiSync has fast convergence with low communication cost.

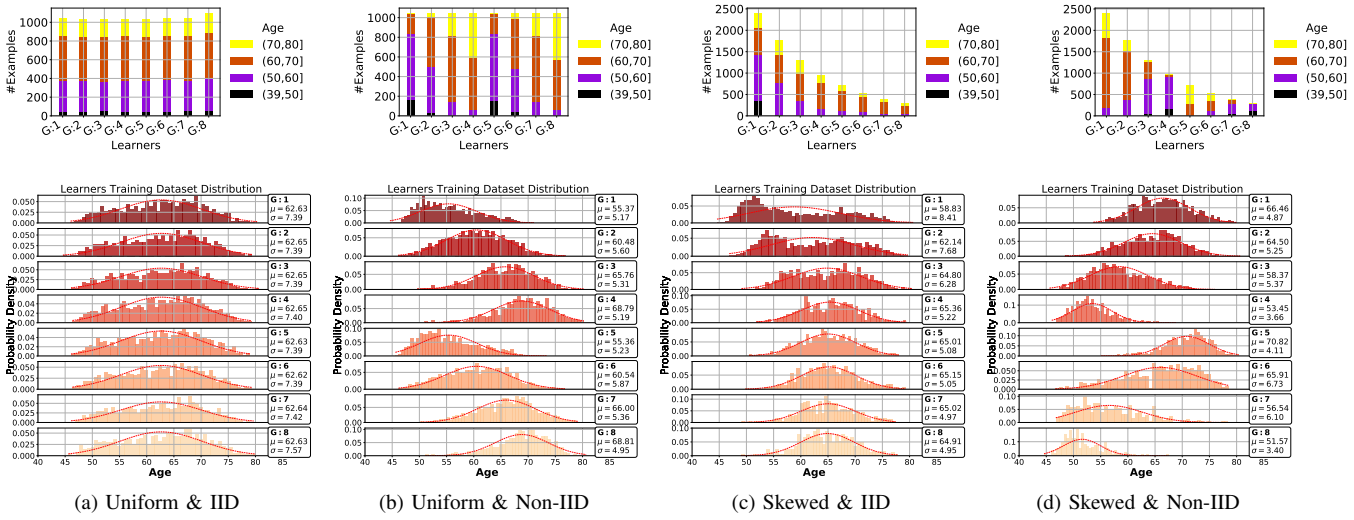


Fig. 2: Heterogenous Federated Learning Environments for the BrainAge Task for a federation of 8 learners with diverse data amounts and age distributions. Age mean and standard deviation for each learner appear next to its subplot.

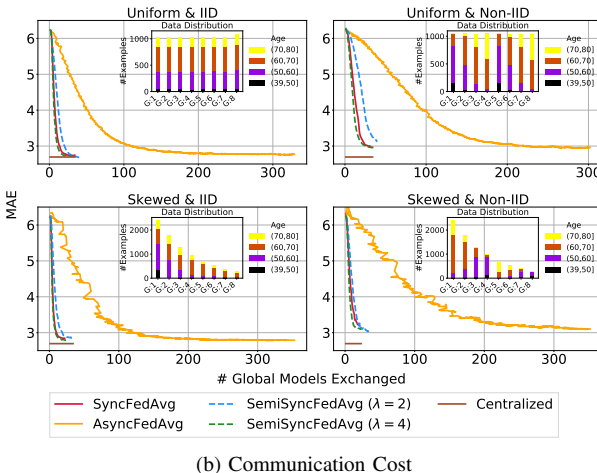
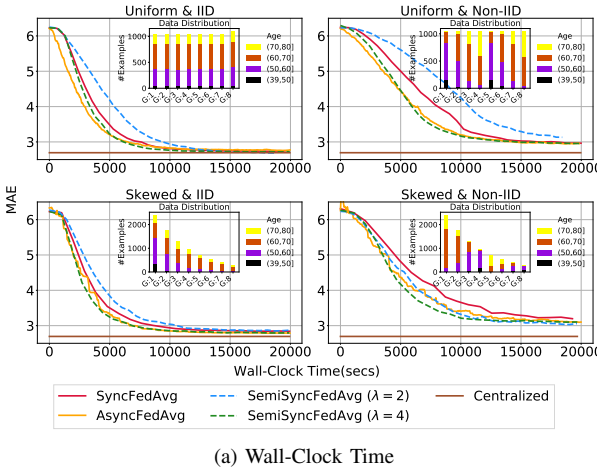


Fig. 3: BrainAGE 3D-CNN model federated learning performance using synchronous, semi-synchronous and asynchronous protocols compared to the best centralized model.

Cohort	Training Set		Test Set	
	Alzheimer's	Controls	Alzheimer's	Controls
ADNI1	1,313	1,832	324	458
ADNI2	384	457	95	115
ADNI3	51	232	13	59
OASIS	36	150	10	38
AIBL	112	641	29	161
<i>Total</i>	<i>1,896</i>	<i>3,312</i>	<i>471</i>	<i>831</i>

TABLE I: AD: Train/test splits per cohort and target label.

B. Predicting Alzheimer's Disease

Dementia affects more than 50 million people worldwide, and this number could exceed 152 million by 2050 [45] with Alzheimer's disease (AD) being the leading cause. Recently, deep learning has been applied to identify AD from structural brain MRI scans [10], [46]–[48].

We study the performance of deep learning for AD prediction in centralized and federated environments. If federated learning achieves comparable performance to centralized training, we posit that, ultimately, federated learning will allow to analyze much greater quantities of data, since it sidesteps many of the challenges of centralized data sharing.

We study 3 prominent AD studies: the Alzheimer's Disease Neuroimaging Initiative (ADNI) [49], with its three phases ADNI1, ADNI2 and ADNI3; the Open Access Series of Imaging Studies (OASIS) [50]; and the Australian Imaging, Biomarkers & Lifestyle Flagship Study of Ageing (AIBL) [51]. These studies contain T1-weighted brain MRI taken from patients with different degrees of dementia and healthy subjects acting as controls. For our work we only use images from control subjects and patients whose cause of dementia is Alzheimer's disease. These studies are longitudinal. To obtain unbiased performance estimates, all the samples for a given subject appear either in the training or in the test set. Table I shows the number of training and testing samples from each study and the target labels.

Images were preprocessed following the pipeline in [46]. First, images were reoriented using `fslreorient2std` (FSL v6.0.1), so to match the orientation of standard template images. Then, brain extraction was performed: skull parts present in the image were removed using the HD-BET CPU implementation, and grey- and white-matter masks were extracted using `FSL-FAST` (FSL v6.0.1 Automated Segmentation Tool). An intensity normalization step (N4 bias field correction) using `ANTs` (v2.2) followed. Next, linear registration to a UK Biobank minimum deformation template was obtained by using the `FSL-FLIRT` (FSL v6.0.1 Linear Image Registration Tool) with 6 degrees of freedom. Finally, an isometric voxel resampling to 2mm was applied using the `ANTs ResampleImage` tool (v2.2). The actual size of the images after the preprocessing were volumes of 91x109x91 voxels.

We trained a 3D-CNN neural model over a federation of 3 (ADNI phases), 4 (ADNI phases + OASIS) and 5 learners (ADNI phases + OASIS + AIBL). Table II shows the performance of the federated and the centralized models. The federated models were trained using the synchronous protocol (i.e., `SyncFedAvg`) for 40 federation rounds with each learner training locally for 4 epochs in-between rounds. The centralized models were trained for 100 epochs with early stopping from epoch 50 to avoid the effects of overfitting. All models were trained using Stochastic Gradient Descent with a learning rate of 2e-4, dropout layers with a dropout rate of 0.2, and L2 weight regularization with $\lambda = 0.1$. All experiments were run 3 times and results show the average and standard deviation of the metrics.

Federated Learning has comparable performance with Centralized training, even though the 5 sites are very heterogeneous in terms of data sizes and proportions of cases versus controls. In fact, federated learning achieves slightly better performance for some metrics and exhibits lower variance in the results, pointing to better generalization.

IV. LEARNING UNDER HOMOMORPHIC ENCRYPTION

Homomorphic Encryption (HE) [52] is a public-key encryption scheme [53] that enables certain computations (e.g., additions, multiplications) to be directly performed over encrypted data without decrypting them first. This distinct computational property renders HE a valuable cryptographic scheme for preserving data privacy in distributed settings, as untrusted parties can be tasked with performing operations over ciphertexts. The element of *homomorphism* derives from the guarantee of following property [54]:

$$Enc(m_1) \odot Enc(m_2) = Enc(m_1 \odot m_2)$$

for some predefined homomorphic operation \odot , and messages $m_1, m_2 \in M$, the message space.

In our work, we specifically employ the Cheon-Kim-Kim-Song (CKKS) fully homomorphic encryption (FHE) scheme [23], which supports arithmetic operations over real and complex data (as opposed to purely integer constructions such as BGV [55], or BFV [56]). CKKS is *fully* homomorphic in that it supports an unbounded amount of arithmetic (or Boolean) circuit operations over encrypted data. FHE is an

intuitive and appropriate tool for securing federated learning environments as it provides strong cryptographic guarantees while still allowing for easy network communication without any underlying access to the plaintext data. The security of CKKS is based on the hardness of the Learning-With-Error (LWE) [57] problem or its ring variant (RLWE [58]). Furthermore, FHE is proven to provide indistinguishability under chosen-plaintext attack (IND-CPA) or *semantic* security.

While CKKS does provide support for real and complex arithmetic, this inherently makes it an *approximate* scheme. This is due to its rescaling operation that drops the least significant bits of computations in order to reduce scaling factors down to their original values during multiplication operations. Formally, this limits ciphertext noise by ensuring the scaling factors remain constant throughout a predefined number of multiplications in order to make compounded homomorphic multiplications much more *efficient*. Additionally, since CKKS largely requires large bit-width integers as input, a residue number system (RNS) variant [59] has been proposed. In this variant, the large integers are broken down into a parallel sets of smaller integers (< 64 bits) involving *residues*, equivalent to the original. The PALISADE lattice-based HE library [60], which we utilize for our work, implements CKKS in this variant for faster computation over 64-bit CPU architectures.

We incorporated the CKKS FHE scheme in our MetisFL Federated Learning architecture. We use homomorphic encryption to communicate the (encrypted) local and global models between the Federation Controller and the learners, and compute the new global model by aggregating learners' local models in encrypted space. Figure 4 presents our federated training pipeline. Training starts with an initial configuration phase, where the Federation Driver generates the homomorphic encryption key pair (private and public key) and the original neural model state. The Federation Controller only receives the model definition and the public key from the driver, since it only needs to perform the private weighted aggregation of local models. The learners, on the contrary, need both the private and public keys during training. The private key is used to decrypt the encrypted global model received by the controller in order to perform their local training (or model evaluation) over their local private dataset, and the public key is used to encrypt the locally trained model prior to being shared with the controller.

We had used a similar training pipeline in [61]. However, in our previous work we encrypted the entire model into a single ciphertext, which created scalability issues for large models. To mitigate this, in MetisFL we encrypt the model on a matrix-by-matrix basis, allowing for a collection of ciphertexts to be communicated between learners and the controller instead of just a single ciphertext. Thereafter, the controller performs the private weighted aggregation over the collection of ciphertexts from all learners. Additionally, we divide the model parameters into batches that are processed in parallel, which leads to a much faster encrypted computation.

We evaluate the learning performance of CKKS on the BrainAGE prediction task over the four federated learning environments presented in Figure 2 using a 3D-CNN model (3 million parameters). The CKKS parameters are multiplicative

Model	Accuracy	Precision	Recall	F1	AUC PR	AUC ROC
ADNI only	0.8570 \pm 0.0090	0.7940 \pm 0.0311	0.8270 \pm 0.0288	0.8095 \pm 0.0080	0.8639 \pm 0.0052	0.8954 \pm 0.0057
OASIS only	0.4428 \pm 0.0194	0.3686 \pm 0.0036	0.7447 \pm 0.0518	0.4927 \pm 0.0091	0.3396 \pm 0.0020	0.4631 \pm 0.0047
AIBL only	0.8050 \pm 0.0044	0.7246 \pm 0.0153	0.7577 \pm 0.0172	0.7405 \pm 0.0022	0.7990 \pm 0.0005	0.8526 \pm 0.0017
Centralized 5AOB	0.8612 \pm 0.0106	0.7977 \pm 0.0350	0.8287 \pm 0.0271	0.8122 \pm 0.0091	0.8683 \pm 0.0130	0.8986 \pm 0.0051
Federated 3A	0.8462 \pm 0.0043	0.8148 \pm 0.0189	0.8048 \pm 0.0194	0.8095 \pm 0.0038	0.8791 \pm 0.0039	0.8967 \pm 0.0012
Federated 4AO	0.8474 \pm 0.0073	0.7955 \pm 0.0126	0.8296 \pm 0.0026	0.8121 \pm 0.0077	0.8766 \pm 0.0007	0.8920 \pm 0.0014
Federated 5AOB	0.8633 \pm 0.0013	0.8098 \pm 0.0043	0.8132 \pm 0.0097	0.8114 \pm 0.0031	0.8682 \pm 0.0009	0.8971 \pm 0.0006

TABLE II: Alzheimer’s Disease Prediction. Test results on a global stratified test dataset (5 sites), for each dataset by itself; 3 sites, ADNI1,2,3 (3A); 4 sites, ADNI1,2,3 + OASIS (4AO), and 5 sites, ADNI1,2,3 + OASIS + AIBL. In federated environments each dataset is at a different learner. Centralized environments are trained over all the corresponding datasets.

depth of 1, 52 scale factor bits, batch size of 4096, and security level of 128 bits. Figure 5 shows the execution (wall-clock) time of synchronous federated average (SyncFedAvg) with and without encryption. Learning performance is almost identical, at a small ($\sim 7\%$) additional training time cost.

V. DEFENDING AGAINST PRIVATE DATA LEAKAGE

Our MetisFL framework uses homomorphic encryption for secure communication and aggregation of parameters. However, each learner needs to decrypt the community model for local training. Therefore, a *curious* site may attempt a *Membership Inference Attacks* [62], [63] by probing the model with local subject data. Discovering that the MRI scan of a particular subject was used for training the model can reveal information about a person’s medical history or participation in some sensitive medical study [64].

We study membership inference attacks in our framework using the white-box experimental setup from Gupta et al. [64]. We assume that the attacker has access to the model, some samples that participated in the training, and some samples the attacker is curious about. We use the same features and architecture as [64] for training models to predict membership. We train the attack model for each learner and compute the accuracy of predicting unseen vs. training samples of all the other learners by creating a balanced set of unseen (i.e., the test samples) and training samples from each learner selected randomly. We report the average of these 56 accuracy values (8 learners and 7 values per learner) as the vulnerability score.

Figure 6 shows the increasing vulnerability of community models at each round. As training progresses, the neural network learns more information about the samples and it becomes easier to identify MRIs participating in training. Previous works [64]–[67] have also found a strong correlation between overfitting and vulnerability to these attacks. We see that data distribution across silos may impact vulnerability. Models trained over more homogenous (IID) data distributions across silos are more vulnerable than heterogenous data distributions (Non-IID), as Non-IID distributions may implicitly regularize and reduce overfitting. Overall, we see that vulnerability increases during training, suggesting a trade-off between learning performance and privacy risk.

The success of privacy attacks is often attributed to the ability of learning algorithms to memorize information about a single sample [68]. Therefore, defending against privacy leakages involves limiting the information that the learning

algorithm may extract about each sample or simply limiting information in the neural network’s weights. We explore two approaches to limit the vulnerability to membership inference attacks: differential private training via DP-SGD [69] and SGD with non-unique gradients.

Differential privacy is a formal framework to reason about privacy. A differential private training mechanism ensures that the outcomes (i.e., final model weights) do not change much between two training sets that differ by one example [70]. For training brain age models with differential privacy guarantees, we use the DP-SGD algorithm [69]. Briefly, the principal modifications to SGD to limit the influence of a single sample are to clip the gradients from each sample not to exceed a maximum norm and to add spherical Gaussian noise. We update each learner during federated training with these private gradients. During initial experiments, we found that achieving non-vacuous differential privacy guarantees requires adding significant Gaussian noise to the gradients, which annihilates learning performance. However, we observed that practical privacy attacks, such as membership inference attacks, can be thwarted by adding Gaussian noise of much smaller magnitudes [71]. Therefore, we evaluate training with gradients with a small additive Gaussian noise.

To learn good machine learning models, we would like to extract patterns while ignoring information about specific samples. Training models using gradient descent can leak an individual’s information during training because there is no restriction on what information a sample may contribute. Thus, the model may preserve information unique to each individual, leaking privacy. Differential privacy adds same noise to all gradients to limit the information or influence of a single sample on the neural network, but that may also destroy useful information in the attempt to reduce memorization. We investigate removing unique information from each sample’s gradient and training with only non-unique parts. We compute the gradient of the loss w.r.t. parameters for each sample in a batch, i.e., $g_i = \nabla_{\theta} L(f(x_i; \theta), y_i) \quad \forall i \in \{1 \dots B\}$. To compute the non-unique part, we project each gradient vector on the subspace spanned by the rest of the gradient vectors (g_i^{span}). We consider the residual part as the unique information about each sample (i.e., $g_i^{unique} = g_i - g_i^{span}$). Ideally, we would like to train with only the non-unique part. However, we observe that it may harm the performance too much, and therefore we downweigh the effect of the unique part and use $\hat{g}_i = g_i^{span} + \alpha g_i^{unique}, \alpha < 1$ to update the

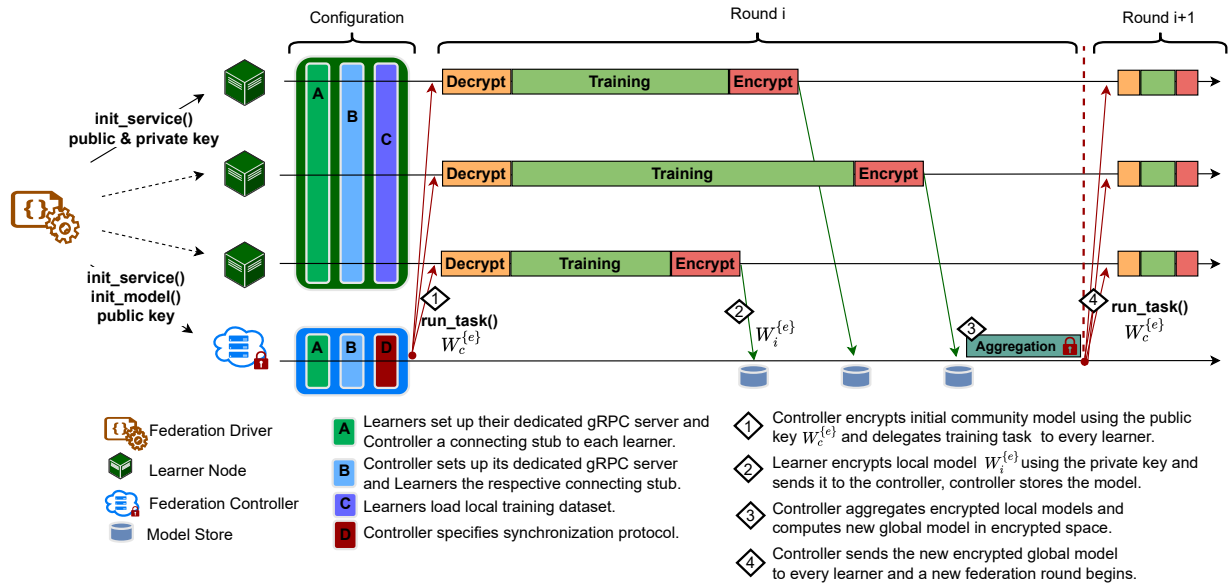


Fig. 4: MetisFL homomorphic encryption training pipeline using the synchronous communication protocol. After the configuration of the federation, controller sends the original encrypted model to each learner, learners decrypt and train the received global model, then encrypt and send the new local model to controller and the controller aggregates the encrypted models, and a new federation round begins.

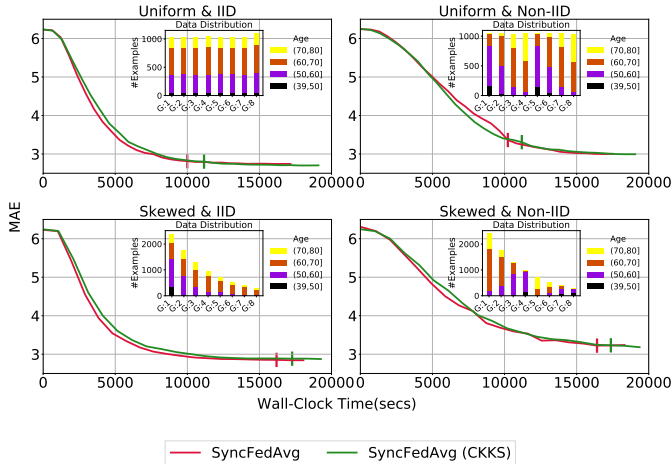


Fig. 5: Federated Learning (SyncFedAvg) with and without CKKS homomorphic encryption on the BrainAge 3D-CNN. The vertical marker represents the training time it takes for each approach to complete 20 federation rounds.

model at local learners. α is a hyperparameter that we tune to trade-off privacy and performance.

Figure 7 shows the privacy and learning performance trade-off when learners are trained with small-magnitude Gaussian noise and our non-unique gradient approach. Both approaches can reduce the vulnerability of model to privacy attacks. Although the magnitude of Gaussian noise is much smaller than the theoretically-required differential privacy guarantees, it effectively reduces membership inference attacks. We hypothesize that the small additive noise is enough to reduce the mutual information between data and neural network outputs/activations, which limits the success of membership

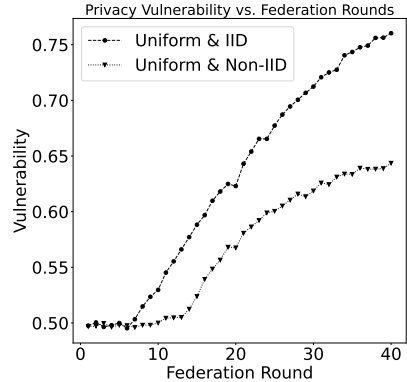


Fig. 6: Privacy vulnerability increases with federation rounds. Vulnerability is measured as the average accuracy of distinguishing train samples vs unseen samples across learners.

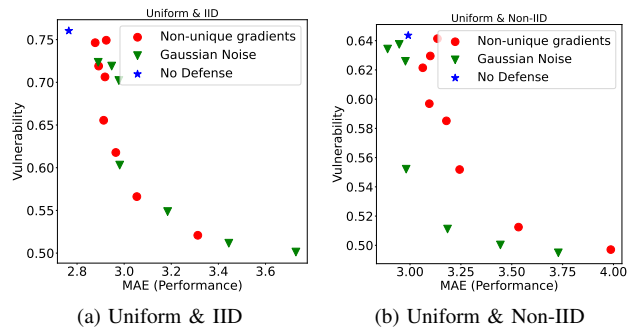


Fig. 7: Vulnerability vs Performance trade-off when training learners with Differential Privacy (Gaussian Noise) and Non-unique gradients approach. Lower vulnerability and lower MAE is desired, i.e., points towards the bottom left are better.

inference attacks [68]. In IID environments, non-unique gradients performs similarly to adding Gaussian noise. However, they are significantly faster to train. The Gaussian noise models required training for 40 rounds, whereas the non-unique gradients required only 25 rounds. In Non-IID environments, training with Gaussian noise provides a better trade-off than non-unique gradients. This may be due to learners overfitting to private datasets earlier in training, thus deviating from the community model. In summary, both small-magnitude Gaussian noise added to Gradients, and non-unique gradients are effective at preventing membership attacks.

VI. RELATED WORK

Federated Learning (FL). Several Federated Learning architectures have recently become available, including Open FL Framework [72], Nvidia Clara, PriMIA [73], Federated AI Technology Enabler (FATE), Flower [74], FedML [75], PySyft [76], FLUTE [77], LEAF [78] and Tensor Flow Federated (TFF). The extensibility, security, and privacy protection of these systems varies. Our focus has been in providing an extensible, modular architecture with strong security via homomorphic encryption and prevention of membership attacks. COINSTAC [79] provides a powerful platform for decentralized neuroimaging analysis. However, their support for training deep learning methods is limited.

Homomorphic Encryption in FL. Truex et al. [80] use a *hybrid* additive homomorphic scheme (Paillier) for private model aggregation. BatchCrypt [81] explores *quantization* schemes for encoding weight updates as a batch and processing them as single instruction multiple data (SIMD) methods through the Pailler scheme. HybridAlpha [82] uses functional encryption (FE) via a secure multi-party communication (SMC) protocol to prevent privacy leakage. FLASHE [83] uses an asymmetric key design limited to only modular addition operations assuming the absence of collusion between any learner and the centralized controller. POSEIDON [84] applies encryption throughout the entire FL process, including local training. EaSTFly [85] combines the use of additive homomorphic encryption (with packing) and Shamir's secret sharing [86], with quantization and ternary gradients for communication reduction. Finally, xMK-CKKS [87] provides a multi-key approach for CKKS, where a public key is aggregated through model decryption once clients share information regarding their individual secret keys.

Privacy in FL. Federated learning avoids sharing datasets. However the exchanged parameters may reveal private information. Various works have highlighted this via practical privacy attacks such as membership inference [62], [63] and model inversion attacks [88], [89], in federated and centralized settings. Researchers have focused on reducing overfitting [66], [67], information in activations and weights [68] or using differential private mechanisms to alleviate such privacy concerns. Learning under differential privacy is particularly attractive as it comes with theoretically solid worst-case guarantees. However, these works assume different threat models, which may relax the problem. For example, [90] assumes that the server can be trusted, whereas [91], [92]

consider a stricter threat model, considering server as honest-but-curious similar to us. Rather than using theoretical upper-bound measure of privacy, we focus on a more practical measure (i.e., membership inference attacks).

VII. DISCUSSION

We introduced the MetisFL Federated Learning framework, an extensible architecture supporting a variety of communication protocols with strong privacy and security mechanisms. We demonstrated its efficacy on Neuroimaging tasks, BrainAGE and Alzheimer's Disease prediction, over challenging computationally and statistically heterogeneous environments. In future work, we plan to investigate training policies to speed-up convergence, supporting additional neural network training engines (e.g., PyTorch), making non-unique gradients robust to Non-IID distributions, and further theoretical analysis of privacy guarantees.

REFERENCES

- [1] M. Wainberg, D. Merico, A. Delong, and B. J. Frey, "Deep learning in biomedicine," *Nature biotechnology*, vol. 36, no. 9, pp. 829–838, 2018.
- [2] K. Suzuki, "Overview of deep learning in medical imaging," *Radiological physics and technology*, vol. 10, no. 3, pp. 257–273, 2017.
- [3] B. Zhu, J. Z. Liu, S. F. Cauley, B. R. Rosen, and M. S. Rosen, "Image reconstruction by domain-transform manifold learning," *Nature*, vol. 555, no. 7697, pp. 487–492, 2018.
- [4] A. V. Dalca, E. Yu, P. Golland, B. Fischl, M. R. Sabuncu, and J. Eugenio Iglesias, "Unsupervised deep learning for bayesian brain mri segmentation," in *International Conference on Medical Image Computing and Computer-Assisted Intervention*. Springer, 2019, pp. 356–365.
- [5] J. Cho, Y. J. Kim, L. Sunwoo, G. P. Lee, T. Q. Nguyen, S. J. Cho, S. H. Baik, Y. J. Bae, B. S. Choi, C. Jung *et al.*, "Deep learning-based computer-aided detection system for automated treatment response assessment of brain metastases on 3d mri," *Frontiers in Oncology*, p. 4314, 2021.
- [6] F. Kofler, C. Berger, D. Waldmannstetter, J. Lipkova, I. Ezhov, G. Tetteh, J. Kirschke, C. Zimmer, B. Wiestler, and B. H. Menze, "Brats toolkit: translating brats brain tumor segmentation algorithms into clinical and scientific practice," *Frontiers in neuroscience*, p. 125, 2020.
- [7] L. M. Aksman, P. A. Wijeratne, N. P. Oxtoby, A. Eshaghi, C. Shand, A. Altmann, D. C. Alexander, and A. L. Young, "pysustain: a python implementation of the subtype and stage inference algorithm," *SoftwareX*, vol. 16, p. 100811, 2021.
- [8] A. L. Young, J. W. Vogel, L. M. Aksman, P. A. Wijeratne, A. Eshaghi, N. P. Oxtoby, S. C. Williams, D. C. Alexander, A. D. N. Initiative *et al.*, "Ordinal sustain: Subtype and stage inference for clinical scores, visual ratings, and other ordinal data," *Frontiers in artificial intelligence*, vol. 4, 2021.
- [9] A. Ezzati, A. Abdulkadir, C. R. Jack Jr, P. M. Thompson, D. J. Harvey, M. Truelove-Hill, L. P. Sreepada, C. Davatzikos, A. D. N. Initiative, and R. B. Lipton, "Predictive value of atn biomarker profiles in estimating disease progression in alzheimer's disease dementia," *Alzheimer's & Dementia*, vol. 17, no. 11, pp. 1855–1867, 2021.
- [10] B. Lu, H.-X. Li, Z.-K. Chang, L. Li, N.-X. Chen, Z.-C. Zhu, H.-X. Zhou, X.-Y. Li, Y.-W. Wang, S.-X. Cui *et al.*, "A practical alzheimer disease classifier via brain imaging-based deep learning on 85,721 samples: A multicentre, retrospective cohort study," *BioRxiv*, pp. 2020–08, 2021.
- [11] P. M. Thompson, N. Jahanshad, C. R. Ching, L. E. Salminen, S. I. Thomopoulos, J. Bright, B. T. Baune, S. Bertolín, J. Bralten, W. B. Bruin *et al.*, "Enigma and global neuroscience: A decade of large-scale studies of the brain in health and disease across more than 40 countries," *Translational psychiatry*, vol. 10, no. 1, pp. 1–28, 2020.
- [12] A. Bischoff-Grethe, I. B. Ozyurt, E. Busa, B. T. Quinn, C. Fennema-Notestine, C. P. Clark, S. Morris, M. W. Bondi, T. L. Jernigan, A. M. Dale *et al.*, "A technique for the deidentification of structural brain MR images," *Human brain mapping*, vol. 28, no. 9, pp. 892–903, 2007.
- [13] N. Schimke and J. Hale, "Quickshear Defacing for Neuroimages," in *Proceedings of the 2nd USENIX conference on Health security and privacy*. USENIX Association, 2011, pp. 11–11.

[14] M. Milchenko and D. Marcus, "Obscuring Surface Anatomy in Volumetric Imaging Data," *Neuroinformatics*, vol. 11, no. 1, pp. 65–75, 2013.

[15] B. McMahan, E. Moore, D. Ramage, S. Hampson, and B. A. y Arcas, "Communication-efficient learning of deep networks from decentralized data," in *Artificial Intelligence and Statistics*. PMLR, 2017, pp. 1273–1282.

[16] Q. Yang, Y. Liu, T. Chen, and Y. Tong, "Federated machine learning: Concept and applications," *ACM Transactions on Intelligent Systems and Technology (TIST)*, vol. 10, no. 2, pp. 1–19, 2019.

[17] T. Li, A. K. Sahu, A. Talwalkar, and V. Smith, "Federated learning: Challenges, methods, and future directions," *IEEE Signal Processing Magazine*, vol. 37, no. 3, pp. 50–60, 2020.

[18] J. Lee, J. Sun, F. Wang, S. Wang, C.-H. Jun, and X. Jiang, "Privacy-preserving patient similarity learning in a federated environment: development and analysis," *JMIR medical informatics*, vol. 6, no. 2, p. e7744, 2018.

[19] M. J. Sheller, G. A. Reina, B. Edwards, J. Martin, and S. Bakas, "Multi-institutional deep learning modeling without sharing patient data: A feasibility study on brain tumor segmentation," in *International MICCAI Brainlesion Workshop*. Springer, 2018, pp. 92–104.

[20] S. Silva, B. A. Gutman, E. Romero, P. M. Thompson, A. Altmann, and M. Lorenzi, "Federated learning in distributed medical databases: Meta-analysis of large-scale subcortical brain data," in *2019 IEEE 16th international symposium on biomedical imaging (ISBI 2019)*. IEEE, 2019, pp. 270–274.

[21] N. Rieke, J. Hancock, W. Li, F. Milletari, H. R. Roth, S. Albarqouni, S. Bakas, M. N. Galtier, B. A. Landman, K. Maier-Hein *et al.*, "The future of digital health with federated learning," *NPJ digital medicine*, vol. 3, no. 1, pp. 1–7, 2020.

[22] S. Silva, A. Altmann, B. Gutman, and M. Lorenzi, "Fed-biomed: A general open-source frontend framework for federated learning in healthcare," in *Domain Adaptation and Representation Transfer, and Distributed and Collaborative Learning*. Springer, 2020, pp. 201–210.

[23] J. H. Cheon, A. Kim, M. Kim, and Y. Song, "Homomorphic encryption for arithmetic of approximate numbers," in *Advances in Cryptology – ASIACRYPT 2017*, T. Takagi and T. Peyrin, Eds., 2017, pp. 409–437.

[24] D. Stripelis and J. L. Ambite, "Accelerating federated learning in heterogeneous data and computational environments," *arXiv:2008.11281*, 2020.

[25] D. Stripelis, M. Abram, and J. L. Ambite, "Performance weighting for robust federated learning against corrupted sources," *arXiv:2205.01184*, 2022.

[26] J. Wang, Z. Charles, Z. Xu, G. Joshi, H. B. McMahan, M. Al-Shedivat, G. Andrew, S. Avestimehr, K. Daly, D. Data *et al.*, "A field guide to federated optimization," *arXiv preprint arXiv:2107.06917*, 2021.

[27] S. J. Reddi, Z. Charles, M. Zaheer, Z. Garrett, K. Rush, J. Konečný, S. Kumar, and H. B. McMahan, "Adaptive federated optimization," in *9th International Conference on Learning Representations, ICLR 2021, Virtual Event, Austria, May 3-7, 2021*. OpenReview.net, 2021. [Online]. Available: <https://openreview.net/forum?id=LkFG3IB13U5>

[28] T.-M. H. Hsu, H. Qi, and M. Brown, "Measuring the effects of non-identical data distribution for federated visual classification," *arXiv preprint arXiv:1909.06335*, 2019.

[29] D. Stripelis, J. L. Ambite, and T. Paul, "Semi-synchronous federated learning for energy-efficient training and accelerated convergence in cross-silo settings," *ACM Transactions on Intelligent Systems and Technology, Special Issue on Federated Learning: Algorithms, Systems, and Applications. Forthcoming*, 2022. [Online]. Available: <https://doi.org/10.1145/3524885>

[30] T. Li, A. K. Sahu, M. Zaheer, M. Sanjabi, A. Talwalkar, and V. Smith, "Federated optimization in heterogeneous networks," in *Proceedings of Machine Learning and Systems*, vol. 2, 2020, pp. 429–450.

[31] C. Xie, S. Koyejo, and I. Gupta, "Asynchronous federated optimization," in *12th Annual Workshop on Optimization for Machine Learning*, 2020.

[32] D. Stripelis, J. L. Ambite, P. Lam, and P. Thompson, "Scaling neuroscience research using federated learning," in *2021 IEEE 18th International Symposium on Biomedical Imaging (ISBI)*. IEEE, 2021, pp. 1191–1195.

[33] K. Franke and C. Gaser, "Ten years of brainage as a neuroimaging biomarker of brain aging: what insights have we gained?" *Frontiers in neurology*, p. 789, 2019.

[34] D. A. Wood, S. Kafabadi, A. Al Busaidi, E. Guilhem, A. Montvila, J. Lynch, M. Townend, S. Agarwal, A. Mazumder, G. J. Barker *et al.*, "Accurate brain-age models for routine clinical mri examinations," *NeuroImage*, p. 118871, 2022.

[35] J. H. Cole, R. Leech, D. J. Sharp, and A. D. N. Initiative, "Prediction of brain age suggests accelerated atrophy after traumatic brain injury," *Annals of neurology*, vol. 77, no. 4, pp. 571–581, 2015.

[36] N. Koutsouleris, C. Davatzikos, S. Borgwardt, C. Gaser, R. Bottlander, T. Frodl, P. Falkai, A. Riecher-Rössler, H.-J. Möller, M. Reiser *et al.*, "Accelerated brain aging in schizophrenia and beyond: a neuroanatomical marker of psychiatric disorders," *Schizophrenia bulletin*, vol. 40, no. 5, pp. 1140–1153, 2014.

[37] A. Kuchinad, P. Schweinhardt, D. A. Seminowicz, P. B. Wood, B. A. Chizh, and M. C. Bushnell, "Accelerated brain gray matter loss in fibromyalgia patients: premature aging of the brain?" *Journal of Neuroscience*, vol. 27, no. 15, pp. 4004–4007, 2007.

[38] P. K. Lam, V. Santhalingam, P. Suresh, R. Baboota, A. H. Zhu, S. I. Thomopoulos, N. Jahanshad, and P. M. Thompson, "Accurate brain age prediction using recurrent slice-based networks," in *16th International Symposium on Medical Information Processing and Analysis*, vol. 11583. International Society for Optics and Photonics, 2020, p. 1158303.

[39] B. A. Jónsson, G. Björnsdóttir, T. Thorgeirsson, L. M. Ellingsen, G. B. Walters, D. Gudbjartsson, H. Stefansson, K. Stefansson, and M. Ulfarsson, "Brain age prediction using deep learning uncovers associated sequence variants," *Nature Communications*, vol. 10, no. 1, pp. 1–10, 2019.

[40] N. K. Dinsdale, E. Bluemke, S. M. Smith, Z. Arya, D. Vidaurre, M. Jenkinson, and A. I. Namburete, "Learning patterns of the ageing brain in mri using deep convolutional networks," *NeuroImage*, vol. 224, p. 117401, 2021.

[41] J. H. Cole, R. P. Poudel, D. Tsagkrasoulis, M. W. Caan, C. Steves, T. D. Spector, and G. Montana, "Predicting brain age with deep learning from raw imaging data results in a reliable and heritable biomarker," *NeuroImage*, vol. 163, pp. 115–124, 2017.

[42] H. Peng, W. Gong, C. F. Beckmann, A. Vedaldi, and S. M. Smith, "Accurate brain age prediction with lightweight deep neural networks," *Medical image analysis*, vol. 68, p. 101871, 2021.

[43] U. Gupta, P. K. Lam, G. Ver Steeg, and P. M. Thompson, "Improved brain age estimation with slice-based set networks," in *2021 IEEE 18th International Symposium on Biomedical Imaging (ISBI)*. IEEE, 2021, pp. 840–844.

[44] K. L. Miller, F. Alfaro-Almagro, N. K. Bangerter, D. L. Thomas, E. Yacoub, J. Xu, A. J. Bartsch, S. Jbabdi, S. N. Sotropoulos, J. L. Andersson *et al.*, "Multimodal population brain imaging in the uk biobank prospective epidemiological study," *Nature neuroscience*, vol. 19, no. 11, pp. 1523–1536, 2016.

[45] C. Patterson, "World alzheimer report 2018," 2018.

[46] N. J. Dhinagar, S. I. Thomopoulos, C. Owens-Walton, D. Stripelis, J. L. Ambite, G. V. Steeg, D. Weintraub, P. Cook, C. McMillan, and P. M. Thompson, "3D convolutional neural networks for classification of Alzheimer's and Parkinson's disease with T1-weighted brain MRI," in *17th International Symposium on Medical Information Processing and Analysis*, L. Rittner, E. R. C. M.D., N. Lepore, J. Brieva, and M. G. Linguraru, Eds., vol. 12088, International Society for Optics and Photonics. SPIE, 2021, pp. 277 – 286. [Online]. Available: <https://doi.org/10.1117/12.2606297>

[47] Y. AbdulAzeem, W. M. Bahgat, and M. Badawy, "A cnn based framework for classification of alzheimer's disease," *Neural Computing and Applications*, vol. 33, no. 16, pp. 10415–10428, 2021.

[48] Y. Fu'adah, I. Wijayanto, N. Pratiwi, F. Taliningsih, S. Rizal, and M. Pramudito, "Automated classification of alzheimer's disease based on mri image processing using convolutional neural network (cnn) with alexnet architecture," in *Journal of Physics: Conference Series*, vol. 1844, no. 1. IOP Publishing, 2021, p. 012020.

[49] S. G. Mueller, M. W. Weiner, L. J. Thal, R. C. Petersen, C. Jack, W. Jagust, J. Q. Trojanowski, A. W. Toga, and L. Beckett, "The alzheimer's disease neuroimaging initiative," *Neuroimaging Clinics*, vol. 15, no. 4, pp. 869–877, 2005.

[50] P. J. LaMontagne, T. L. Benzinger, J. C. Morris, S. Keefe, R. Hornbeck, C. Xiong, E. Grant, J. Hassenstab, K. Moulder, A. G. Vlassenko, M. E. Raichle, C. Cruchaga, and D. Marcus, "Oasis-3: Longitudinal neuroimaging, clinical, and cognitive dataset for normal aging and alzheimer disease," *medRxiv*, 2019. [Online]. Available: <https://www.medrxiv.org/content/early/2019/12/15/2019.12.13.19014902>

[51] C. Fowler, S. R. Rainey-Smith, S. Bird, J. Bomke, P. Bourgeat, B. M. Brown, S. C. Burnham, A. I. Bush, C. Chadunow, S. Collins *et al.*, "Fifteen years of the australian imaging, biomarkers and lifestyle (aibl) study: progress and observations from 2,359 older adults spanning the spectrum from cognitive normality to alzheimer's disease," *Journal of Alzheimer's disease reports*, no. Preprint, pp. 1–26, 2021.

[52] M. Albrecht, M. Chase, H. Chen, J. Ding, S. Goldwasser, S. Gorbunov, S. Halevi, J. Hoffstein, K. Laine, K. Lauter, S. Lokam, D. Micciancio, D. Moody, T. Morrison, A. Sahai, and V. Vaikuntanathan, “Homomorphic encryption security standard,” HomomorphicEncryption.org, Toronto, Canada, Tech. Rep., November 2018.

[53] K. Sako, *Public Key Cryptography*. Boston, MA: Springer US, 2011, pp. 996–997.

[54] A. Acar, H. Aksu, A. S. Uluagac, and M. Conti, “A survey on homomorphic encryption schemes: Theory and implementation,” 2017.

[55] Z. Brakerski, C. Gentry, and V. Vaikuntanathan, “(leveled) fully homomorphic encryption without bootstrapping,” in *Proceedings of the 3rd Innovations in Theoretical Computer Science Conference*, ser. ITCS ’12. Association for Computing Machinery, 2012, p. 309–325.

[56] J. Fan and F. Vercauteren, “Somewhat practical fully homomorphic encryption,” *IACR Cryptol. ePrint Arch.*, p. 144, 2012.

[57] O. Regev, “On lattices, learning with errors, random linear codes, and cryptography,” *J. ACM*, vol. 56, no. 6, Sep. 2009. [Online]. Available: <https://doi.org/10.1145/1568318.1568324>

[58] V. Lyubashevsky, C. Peikert, and O. Regev, “On ideal lattices and learning with errors over rings,” vol. 60, no. 6, Nov. 2013. [Online]. Available: <https://doi.org/10.1145/2535925>

[59] J. H. Cheon, K. Han, A. Kim, M. Kim, and Y. Song, “A full rns variant of approximate homomorphic encryption,” in *International Conference on Selected Areas in Cryptography*. Springer, 2018, pp. 347–368.

[60] Y. Polyakov, K. Rohloff, and G. W. Ryan, “Palisade lattice cryptography library user manual,” *Cybersecurity Research Center, New Jersey Institute of Technology (NJIT), Tech. Rep.*, vol. 15, 2017.

[61] D. Stripelis, H. Saleem, T. Ghai, N. Dhinagar, U. Gupta, C. Anastasiou, G. Ver Steeg, S. Ravi, M. Naveed, P. M. Thompson *et al.*, “Secure neuroimaging analysis using federated learning with homomorphic encryption,” in *17th International Symposium on Medical Information Processing and Analysis*, vol. 12088. SPIE, 2021, pp. 351–359.

[62] R. Shokri, M. Stronati, C. Song, and V. Shmatikov, “Membership Inference Attacks Against Machine Learning Models,” in *2017 IEEE Symposium on Security and Privacy (SP)*, 2017, pp. 3–18.

[63] M. Nasr, R. Shokri, and A. Houmansadr, “Comprehensive Privacy Analysis of Deep Learning: Passive and Active White-box Inference Attacks against Centralized and Federated Learning,” in *2019 IEEE Symposium on Security and Privacy (SP)*, 2019, pp. 739–753.

[64] U. Gupta, D. Stripelis, P. K. Lam, P. Thompson, J. L. Ambite, and G. Ver Steeg, “Membership inference attacks on deep regression models for neuroimaging,” in *Medical Imaging with Deep Learning*. PMLR, 2021, pp. 228–251.

[65] S. Yeom, I. Giacomelli, M. Fredrikson, and S. Jha, “Privacy risk in machine learning: Analyzing the connection to overfitting,” in *2018 IEEE 31st computer security foundations symposium (CSF)*. IEEE, 2018, pp. 268–282.

[66] S. Truex, L. Liu, M. E. Gursoy, L. Yu, and W. Wei, “Towards Demystifying Membership Inference Attacks,” *arXiv preprint arXiv:1807.09173*, 2018.

[67] A. Salem, Y. Zhang, M. Humbert, M. Fritz, and M. Backes, “ML-Leaks: Model and Data Independent Membership Inference Attacks and Defenses on Machine Learning Models,” in *Network and Distributed Systems Security Symposium 2019*. Internet Society, 2019.

[68] S. K. Jha, S. Jha, R. Ewetz, S. Raj, A. Velasquez, L. L. Pullum, and A. Swami, “An Extension of Fano’s Inequality for Characterizing Model Susceptibility to Membership Inference Attacks,” *arXiv preprint arXiv:2009.08097*, 2020.

[69] M. Abadi, A. Chu, I. Goodfellow, H. B. McMahan, I. Mironov, K. Talwar, and L. Zhang, “Deep Learning with Differential Privacy,” in *Proceedings of the 2016 ACM SIGSAC conference on computer and communications security*, 2016, pp. 308–318.

[70] C. Dwork and A. Roth, “The Algorithmic Foundations of Differential Privacy,” *Foundations and Trends® in Theoretical Computer Science*, vol. 9, no. 3–4, pp. 211–407, 2014.

[71] B. Jayaraman and D. Evans, “Evaluating Differentially Private Machine Learning in Practice,” in *28th USENIX Security Symposium (USENIX Security 19)*. USENIX Association, 2019, pp. 1895–1912.

[72] G. A. Reina, A. Gruzdev, P. Foley, O. Perepelkina, M. Sharma, I. Davyduk, I. Trushkin, M. Radionov, A. Mokrov, D. Agapov *et al.*, “Openfl: An open-source framework for federated learning,” *arXiv preprint arXiv:2105.06413*, 2021.

[73] G. Kaassis, A. Ziller, J. Passerat-Palmbach, T. Ryffel, D. Usynin, A. Trask, I. Lima, J. Mancuso, F. Jungmann, M.-M. Steinborn *et al.*, “End-to-end privacy preserving deep learning on multi-institutional medical imaging,” *Nature Machine Intelligence*, vol. 3, no. 6, pp. 473–484, 2021.

[74] D. J. Beutel, T. Topal, A. Mathur, X. Qiu, J. Fernandez-Marques, Y. Gao, L. Sani, K. H. Li, T. Parcollet, P. P. B. de Gusmão *et al.*, “Flower: A friendly federated learning framework,” *arXiv preprint arXiv:2007.14390*, 2022.

[75] C. He, S. Li, J. So, X. Zeng, M. Zhang, H. Wang, X. Wang, P. Vepakomma, A. Singh, H. Qiu *et al.*, “Fedml: A research library and benchmark for federated machine learning,” *arXiv preprint arXiv:2007.13518*, 2020.

[76] A. Ziller, A. Trask, A. Lopardo, B. Szymkow, B. Wagner, E. Bluemke, J.-M. Nounahon, J. Passerat-Palmbach, K. Prakash, N. Rose *et al.*, “Pysyft: A library for easy federated learning,” in *Federated Learning Systems*. Springer, 2021, pp. 111–139.

[77] D. Dimitriadis, M. H. Garcia, D. M. Diaz, A. Manoel, and R. Sim, “Flute: A scalable, extensible framework for high-performance federated learning simulations,” *arXiv preprint arXiv:2203.13789*, 2022.

[78] S. Caldas, S. M. K. Duddu, P. Wu, T. Li, J. Konečný, H. B. McMahan, V. Smith, and A. Talwalkar, “Leaf: A benchmark for federated settings,” *arXiv preprint arXiv:1812.01097*, 2018.

[79] S. M. Plis, A. D. Sarwate, D. Wood, C. Dieringer, D. Landis, C. Reed, S. R. Panta, J. A. Turner, J. M. Shoemaker, K. W. Carter *et al.*, “Cointstac: a privacy enabled model and prototype for leveraging and processing decentralized brain imaging data,” *Frontiers in neuroscience*, vol. 10, p. 365, 2016.

[80] S. Truex, N. Baracaldo, A. Anwar, T. Steinke, H. Ludwig, and R. Zhang, “A hybrid approach to privacy-preserving federated learning,” *CoRR*, vol. abs/1812.03224, 2018. [Online]. Available: <http://arxiv.org/abs/1812.03224>

[81] C. Zhang, S. Li, J. Xia, W. Wang, F. Yan, and Y. Liu, “Batchcrypt: Efficient homomorphic encryption for cross-silo federated learning,” in *2020 USENIX Annual Technical Conference (USENIX ATC 20)*. USENIX Association, Jul. 2020, pp. 493–506. [Online]. Available: <https://www.usenix.org/conference/atc20/presentation/zhang-chengliang>

[82] R. Xu, N. Baracaldo, Y. Zhou, A. Anwar, and H. Ludwig, “Hybridalpha: An efficient approach for privacy-preserving federated learning,” in *Proceedings of the 12th ACM Workshop on Artificial Intelligence and Security, AISec@CCS 2019, London, UK, November 15, 2019*, L. Cavallaro, J. Kinder, S. Afroz, B. Biggio, N. Carlini, Y. Elovici, and A. Shabtai, Eds. ACM, 2019, pp. 13–23. [Online]. Available: <https://doi.org/10.1145/3338501.3357371>

[83] Z. Jiang, W. Wang, and Y. Liu, “FLASHE: additively symmetric homomorphic encryption for cross-silo federated learning,” *CoRR*, vol. abs/2109.00675, 2021. [Online]. Available: <https://arxiv.org/abs/2109.00675>

[84] S. Sav, A. Pyrgelis, J. R. Troncoso-Pastoriza, D. Froelicher, J. Bossuat, J. S. Sousa, and J. Hubaux, “POSEIDON: privacy-preserving federated neural network learning,” *CoRR*, vol. abs/2009.00349, 2020. [Online]. Available: <https://arxiv.org/abs/2009.00349>

[85] Y. Dong, X. Chen, L. Shen, and D. Wang, “Eastfly: Efficient and secure ternary federated learning,” *Computers & Security*, vol. 94, p. 101824, 2020. [Online]. Available: <https://www.sciencedirect.com/science/article/pii/S0167404820300985>

[86] A. Shamir, “How to share a secret,” *Commun. ACM*, vol. 22, no. 11, p. 612–613, nov 1979. [Online]. Available: <https://doi.org/10.1145/359168.359176>

[87] J. Ma, S.-A. Naas, S. Sigg, and X. Lyu, “Privacy-preserving federated learning based on multi-key homomorphic encryption,” *International Journal of Intelligent Systems*, 2022.

[88] J. Geiping, H. Bauermeister, H. Dröge, and M. Moeller, “Inverting gradients-how easy is it to break privacy in federated learning?” *Advances in Neural Information Processing Systems*, vol. 33, pp. 16 947–16 947, 2020.

[89] L. Zhu, Z. Liu, and S. Han, “Deep leakage from gradients,” *Advances in Neural Information Processing Systems*, vol. 32, 2019.

[90] K. Wei, J. Li, M. Ding, C. Ma, H. H. Yang, F. Farokhi, S. Jin, T. Q. Quek, and H. V. Poor, “Federated learning with differential privacy: Algorithms and performance analysis,” *IEEE Transactions on Information Forensics and Security*, vol. 15, pp. 3454–3469, 2020.

[91] M. Noble, A. Bellet, and A. Dieuleveut, “Differentially private federated learning on heterogeneous data,” *arXiv preprint arXiv:2111.09278*, 2021.

[92] Y. Zhao, J. Zhao, M. Yang, T. Wang, N. Wang, L. Lyu, D. Niyato, and K.-Y. Lam, “Local differential privacy-based federated learning for internet of things,” *IEEE Internet of Things Journal*, vol. 8, no. 11, pp. 8836–8853, 2020.